JACS
JOURNAL OF THE AMERICAN CHEMICAL SOCIETY

Article

pubs.acs.org/JACS

Organic Dye-Sensitized Tandem Photoelectrochemical Cell for Light Driven Total Water Splitting

Fusheng Li,[†] Ke Fan,[†] Bo Xu,[†] Erik Gabrielsson,[†] Quentin Daniel,[†] Lin Li,[†] and Licheng Sun*[,†,‡]

[†]Department of Chemistry, KTH Royal Institute of Technology, 110044 Stockholm, Sweden

[‡]State Key Laboratory of Fine Chemicals, DUT−KTH Joint Education and Research Center on Molecular Devices Dalian University of Technology (DUT), Dalian 116024, P. R. China

Supporting Information

ABSTRACT: Light driven water splitting was achieved by a tandem dye-sensitized photoelectrochemical cell with two photoactive electrodes. The photoanode is constituted by an organic dye **L0** as photosensitizer and a molecular complex **Ru1** as water oxidation catalyst on meso-porous TiO_2, while the photocathode is constructed with an organic dye **P1** as photoabsorber and a molecular complex **Co1** as hydrogen generation catalyst on nanostructured NiO. By combining the photocathode and the photoanode, this tandem DS-PEC cell can split water by visible light under neutral pH conditions without applying any bias.

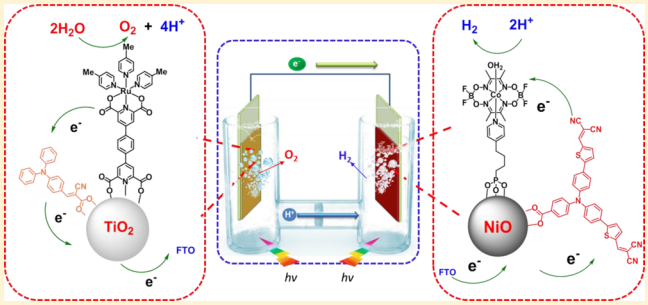

INTRODUCTION

To satisfy our society's global sustainable energy demands, utilizing solar energy to split water to produce hydrogen by photoelectrochemical (PEC) cell is one of the most promising strategies.[1−3] Molecular catalysts have shown great potential for the development of highly efficient water splitting devices due to their easy modification in structures, fine-tuning in redox properties, and high catalytic efficiencies.[4−8] Recently, a series of molecular PEC cells for water splitting have been developed in our group.[9−12] In these devices, $Ru(bpy)_3$-type photosensitizers were used together with molecular catalysts on TiO_2 as the photoanodes, and Pt as the cathode. In order to avoid the use of expensive metal Pt, a tandem molecular PEC cell was developed by our group,[13] which showed a steady photocurrent density for water splitting under neutral pH conditions. This study indicates that Pt-free tandem molecular PEC cells can achieve total water splitting driven by visible light. However, the high cost of the Ru-based photosensitizer is another limitation for the future large-scale application of this type of device. Metal-free organic dyes have been widely used in dye-sensitized solar cells (DSSCs) due to their high efficiency, easy modification, tunable electron transfer process, and low cost, which can be considered as the alternatives for Ru-based photosensitizers in PEC devices.[14] Recently, Finke et al. published an encouraging work in which perylene diimide served as an n-type semiconductor to drive CoO_X for water oxidation, and a photocurrent of 150 μA cm^{-2} was obtained,[15] but a very high bias was required (1 V vs Ag/AgCl) for this photoanode. Later, Mallouk et al. demonstrated a photoanode in which porphyrin dyes were used as photosensitizers to drive IrO_X for water oxidation, but the photocurrent density (less 50 μA cm^{-2}) and stability were not satisfactory.[16] So far, no organic molecule showing better performance than $Ru(bpy)_3$-based dye for light-driving water splitting in PEC devices has been reported. Herein, we report a tandem PEC cell for total water splitting under neutral pH conditions, in which the photoanode is cosensitized by a simple organic dye **L0** and Ru-based catalyst **Ru1** on *meso*-TiO_2, and the photocathode employs an organic dye **P1** and Co-based catalysts **Co1** cosensitized on NiO, as shown in Scheme 1. This is the first case that organic dyes are employed as photosensitizers in both photoanode and photocathode of a tandem molecular PEC device for light driven over all water splitting.

Scheme 1. Representation of the Photoanode with Organic Dye L0 and Catalyst Ru1 on TiO_2, and the Photocathode with Organic Dye P1 and Catalyst Co1 on NiO

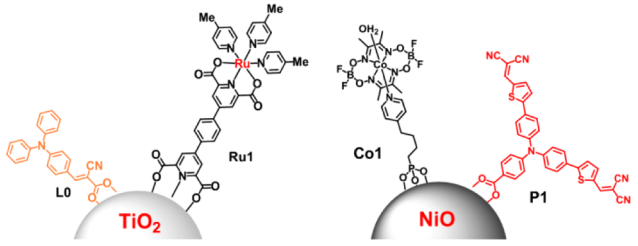

To make rational design of a tandem DS-PEC cell, several key issues should be considered: (i) the energy gap of the photoanode and the photocathode should match with each other. Here, we use TiO_2 as the photoanode material and NiO

Received: May 10, 2015
Published: July 1, 2015

ACS Publications © 2015 American Chemical Society

DOI: 10.1021/jacs.5b04856
J. Am. Chem. Soc. 2015, 137, 9153−9159

Table 1. Optical and Electrochemical Properties of the Dyes and Catalysts

dyes and catalysts	λ_{abs} (ε/M^{-1} cm^1)/nm	λ_{em}/nm	E_{ox} (HOMO)/V vs NHE	E_{0-0}/eV	LUMO/V vs NHE
P1	348(34720);481(57900)	618	1.32	2.25	− 0.93
L0	373 387(36000)	509	1.37	2.90	−1.53
Ru1	**Ru1** onset potential for water oxidation on TiO_2 is around 1.20 V				
Co1	**Co1** onset potential for hydrogen generation on NiO is around −0.54 V				

as the photocathode material, which is similar to the design of tandem *pn*-DSSCs;[17] (ii) the excited state of the n-type dye can inject an electron into the conduction band (CB) of TiO_2 from its lowest unoccupied molecular orbital (LUMO), while the excited state of the p-type dye can inject a hole into the valence band (VB) of NiO from its highest occupied molecular orbital (HOMO); (iii) for the photoanode, the dye's oxidation potential, E_{ox}, should be more positive than the onset potential of water oxidation catalyst (WOC); whereas for the photocathode, the dye's reduction potential, E_{red}, should be more negative than the onset potential of hydrogen generation catalyst (HGC); (iv) according to our previous study,[11] the distance between the dye and the surface of semiconductor should be shorter than the distance between the catalyst and the surface of semiconductor to facilitate the desired electron/hole injection and subsequent electron transfer.

Following the above considerations, the WOC **Ru1** [Ru(pdc)(pic)$_3$ with pyridine-2,6-dicarboxylic acid (pdc) as an anchoring group, pic = 4-picoline] and the organic dye **L0** were immobilized on the surface of n-type TiO_2 film (8 μm thickness) for making the photoanode. Considering that the organic dyes may form aggregates (dye island formation) and affect the device performance, the catalyst **Ru1** was adsorbed on TiO_2 first, followed by the adsorption of **L0**. The loading amount of catalyst **Ru1** can be controlled by changing the concentration of **Ru1** and the loading time. Correspondingly, the HGC **Co1** [$Co(dmgBF_2)_2(H_2O)$ with phosphonic acid as an anchoring group, $dmgBF_2$ = difluoroboryldimethylglyoximato] and the organic dye **P1** were immobilized on the surface of p-type NiO for the photocathode.

EXPERIMENTAL SECTION

Materials. All chemicals and solvents, if not otherwise stated, were purchased from Sigma-Aldrich and used without further purification; the water used in syntheses and measurements was deionized by Milli-Q technique. 4-Hydroxy-2,6-pyridinedicarboxylic acid and 4-methylpyridine were purchased from TCI Development Co., Ltd. *cis*-$Ru(DMSO)_4Cl_2$ and $Co(dmgBF_2)_2(H_2O)_2$ were prepared according to published methods.[18,19] Synthetic routes of **Ru1** and **Co1** can be found in the Supporting Information (SI).

General Electrochemical Methods. All electrochemical measurements were carried out using an Autolab potentiostat with a GPES electrochemical interface (Eco Chemie). Ag/AgCl in 3 M KCl and platinum foil were used as the reference electrode and the counter electrode, respectively. Using this reference electrode, all the potentials were converted to NHE using the $[Ru(bpy)_3]^{2+}/[Ru(bpy)_3]^{3+}$ couple (Half-wave potential $E_{1/2}$ = 1.26 V vs NHE) as an internal reference. $E_{1/2}$ was determined by cyclic voltammetry as the average of the anodic and cathodic peak potentials ($E_{1/2} = (E_{pa} + E_{pc})/2$). To measure the electrochemical properties of catalysts on the metal oxide films, mix films were used due to the nature of TiO_2 and NiO. TiO_2+ITO (ITO = indium tin oxide, mass ratio 1:4) and NiO+ITO (mass ratio 1:4) were spin coated on FTO glasses, the films were calcinated at 450 °C for 2 h, then TiO_2+ITO film and NiO+ITO film were dipped into **Ru1** solution, and **Co1** solution for 1 h respectively, **Ru1**@TiO_2+ITO and **Co1**@NiO+ITO electrodes were thus obtained.

Preparation of Photoanode and Photocathode. TiO_2 and NiO films were prepared according to our previous reports.[10,20] The thicknesses of the obtained bare TiO_2 film and NiO film are ca. 8 and 1 μm, respectively. The active areas of the photoelectrodes were 1 cm^2. The bare TiO_2 film was dipped into 1 mM **Ru1** DCM (dichloromethane) solution for 15 min, after being rinsed by MeOH, the film was immersed in 1 mM **L0** DCM solution for 1 h. The bare NiO film was dipped into 1 mM **P1** DCM solution for 5 min. After being rinsed by MeOH, the film was immersed in 1 mM **Co1** for 1 h. The electrodes without loading photosensitizers or catalysts were prepared as well by using the same procedure as references.

Photoelectrochemical Measurements. Photoelectrochemical measurements were carried out in phosphate buffer solution (pH 7, 50 mM Sigma-Aldrich). In order to compare it with our previous work,[21] all tests were operated under a light source of white LED light (λ > 400 nm, Color temperature 6000−6500 K, light intensity 100 mW cm^{-2}). To investigate the molecular photoanode and photocathode separately, conventional PEC cells were constructed using photoanode or photocathode as the working electrode, Pt net as the counter electrode, and Ag/AgCl electrode (3 M KCl) as the reference electrode. All of the PEC cells were degassed by Ar or N_2 for 20 min before the photoelectrochemical measurements.

Determination of O_2 Generation. The electrolyte in the PEC device was thoroughly degassed by N_2. The volumes of the solution and the headspace in the working compartment were measured. To evaluate oxygen generation, a 0.5 mL gas phase of the headspace was transferred into a gas chromatograph (GC) using a Hamilton SampleLock syringe. A GC-2014, Shimadzu Molecular sieve 5A, TCD detector, with nitrogen as the carrying gas was used to measure the H_2 evolution, and with helium as a carrier gas was used to measure the O_2 evolution.

IPCE Measurements. Incident photon to current conversion efficiency (IPCE) spectra were obtained by illumination of the photoelectrodes with light of a specific wavelength (from 370 to 650 nm) and measuring the resulting short-circuit current. The currents were recorded using a computer-controlled setup consisting of potentiostat (EG&GPAR 273). The illumination was supplied by a Xenon light source (Spectral Products ASB-XE-175) and calibrated using a certified reference solar cell (Fraunhofer ISE). The specific wavelength was controlled by a monochromator (Spectral Products CM110).

RESULTS AND DISCUSSION

From cyclic voltammetry curves of **Ru1**@TiO_2+ITO and **Co1**@NiO+ITO electrodes (SI Figure S4 and S5), the onset potentials of WOC and HGC can be determined, the E_{onset} of **Ru1** for water oxidation is around 1.2 V vs NHE, and the E_{onset} of **Co1** for hydrogen generation is around −0.54 V vs NHE. The organic dyes **L0** and **P1** have been reported in DSSCs.[22−24] Corresponding optical and electrochemical properties of the dyes and the catalysts are shown in Table 1.

According to the electrochemical properties of the dyes, catalysts, and semiconductors,[17,25] a schematic energy diagram was illustrated in Scheme 2. After illumination of the photoanode, the excited state of dye **L0** can inject an electron into the CB of TiO_2, and the photogenerated **L0**$^+$ can oxidize the catalyst **Ru1**, leading to water oxidation after repeated multielectron transfer processes. Meanwhile, at the photocathode, the excited state **P1** can inject holes into the VB of NiO and the formed **P1**$^-$, which can reduce the catalyst **Co1** for eventual hydrogen generation.

DOI: 10.1021/jacs.5b04856
J. Am. Chem. Soc. 2015, 137, 9153−9159

Scheme 2. Schematic Energy Diagram for L0, P1, Ru1, Co1, FTO, TiO_2, and NiO (All Data Shown at pH 7)

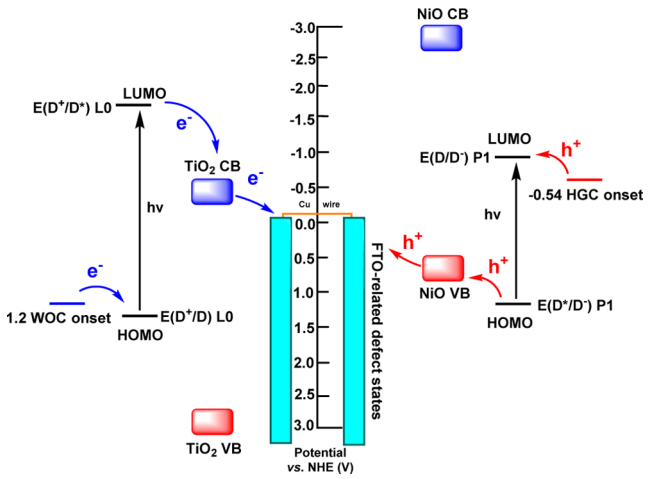

First, linear scan voltammetry (LSV) of **L0+Ru1**@TiO_2 under illumination (Figure 1) showed that the photocurrent

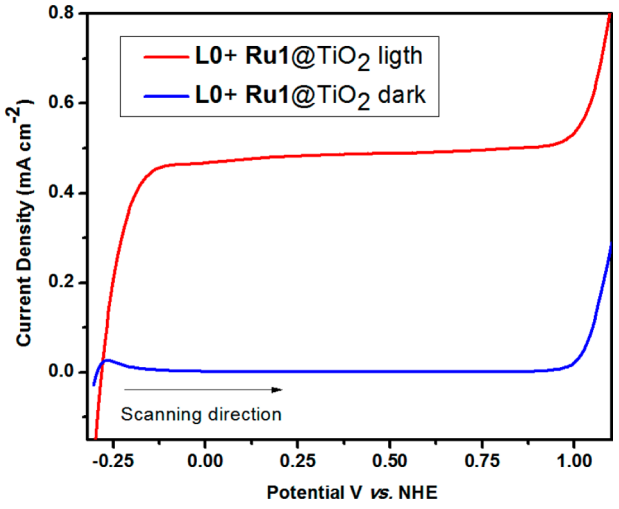

Figure 1. LSV measurements of the WEs under light illumination (light intensity 100 mW cm^{-2}) and scan rate = 50 mV s^{-1}, in a **three-electrode** PEC cell with Pt as counter electrode and Ag/AgCl as reference electrode, operated in a 50 mM pH 7.0 phosphate buffer solution.

rapidly increased with the applied potential from −0.25 to −0.15 V (vs NHE), and reached a plateau at $E > -0.1$ V with a photocurrent density of 0.42 mA cm^{-2}. This value is significantly higher in comparison to the current densities under dark conditions, indicating that the working electrode is indeed photoactive. From LSV, the relationship between the applied bias potential and the photocurrent can be found, here 0 V vs Ag/AgCl as the applied bias was selected to measure the photocurrent of **L0+Ru1**@TiO_2 electrode.

Transient current responses to on−off cycles and full-time photocurrent under illumination were then studied, and the results are shown in Figure 2. For the **L0+Ru1**@TiO_2 photoanode, it produced a remarkable average photocurrent of ca. 300 μA cm^{-2}. For the **L0**@TiO_2 photoanode without the catalyst **Ru1**, it only produced ca. 30 μA cm^{-2} photocurrent density under the same conditions, while for **Ru1**@TiO_2 electrode, only an indistinct photocurrent can be achieved (SI

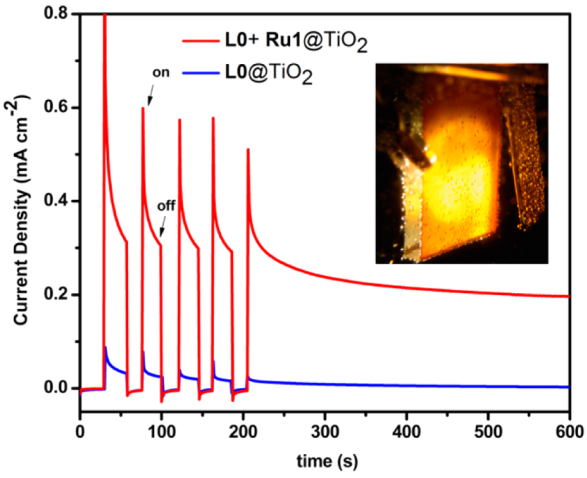

Figure 2. Transient current responses to on−off cycles and full time photocurrent of illumination (light intensity 100 mW cm^{-2}) on photoanodes under an applied bias potential of 0 V vs Ag/AgCl in a **three-electrode** PEC cell with Pt as counter electrode, operated in a 50 mM pH 7.0 phosphate buffer solution.

Figure S8). **Ru1** has a strong absorption of visible light (SI Figure S6), but it will be hard for **Ru1** to inject 4 electrons into TiO_2 and generate Ru^V species for water oxidation. The significant increase of photocurrent confirms the highly catalytic activity of **Ru1** for water oxidation, and the electron transfer from the catalyst to the oxidized dye should occur as anticipated. In comparison to our previous study on similar PEC devices using the catalyst **Ru1** and $Ru(bpy)_3$-based photosensitizer on TiO_2 as photoanode (giving a photocurrent density of ca. 100 μA cm^{-2}),[13] the higher photocurrent density obtained from the photoanode **L0+Ru1**@TiO_2 indicates that this simple organic dye **L0** based device exhibits much better device performance than the expensive $Ru(bpy)_3$ photosensitizer based device. Additionally, compared to the photoanodes developed by Finke and Mallouk,[15,16] our photoande **L0+Ru1**@TiO_2 shows advances of low applied bias potential and high current density.

In a long-term illumination experiment, the photoanode **L0+Ru1**@TiO_2 showed a relatively slow decay of photocurrent (Figure 2 and SI Figure S10). It is well-known that the stability of molecular PEC cells is usually poor.[10−12] One of the main reasons is that molecular catalysts or dyes can detach from the metal oxide surface in the presence of electrolyte solution, which leads to a drastic decay of the photocurrent. In our case, pyridine-2,6-dicarboxylic acid was used as the anchoring group of the catalyst **Ru1**, which is exceptionally strong in comparison to the commonly used carboxylic acid and phosphonic acid,[13,26] no obvious desorption of the catalyst **Ru1** from the surface of TiO_2 can be observed with pHs ranging from 1 to 14. The organic dye **L0** is insoluble in water, which can also hinder the desorption from the surface of TiO_2. Due to these reasons, our photoanode **L0+Ru1**@TiO_2 shows a much better stability.

During 60 min illumination, bubbles were formed on the photoanode surface (inset of Figure 2 and SI Figure S9), the photogenerated oxygen gas was confirmed by gas chromatography (GC), 0.46 C charges passed through the electrode (SI Figure S10), 0.87 μmol O_2 was detected by GC, and the Faraday efficiency was calculated to be 73%. More interestingly, with the long time illumination on the photoanode in the two-electrode system (**L0+Ru1**@TiO_2 0.4 cm^2 as working electrode

DOI: 10.1021/jacs.5b04856
J. Am. Chem. Soc. 2015, 137, 9153−9159

and Pt net as counter electrode) without applying any bias, the PEC cell can still generate oxygen, which was detected by Clark-electrode (SI Figure S11). For the photoanode with **L0** alone (**L0**@TiO_2), only 15 nmol mL^{-1} oxygen was generated after 30 min illumination. For the photoanode with **Ru1** alone, almost no oxygen can be detected. In contrast, for the **L0**+**Ru1**@TiO_2 electrode, 140 nmol mL^{-1} oxygen was obtained after 30 min illumination. These results clearly prove that the light-driven water oxidation is successfully achieved by assembly with catalyst **Ru1** and organic photosensitizer **L0** on TiO_2.

For preparing the photocathode, a cobalt complex **Co1** with an anchoring group was employed as the hydrogen generation catalyst and organic dye **P1** was used as photosensitizer, and they were immobilized on NiO film. Since the NiO film used here was very thin (1 μm in thickness), **P1** was adsorbed before **Co1** to make sure more dyes can be loaded on the electrode. LSV experiments on the assembled **P1**+**Co1**@NiO photocathode show that, under illumination, the photocurrent rapidly increased with the applied potential from 0.4 to −0.1 V (vs. NHE), and reached a plateau at E < −0.1 V with a photocurrent density of ca. −45 μA cm^{-2} (Figure 3).

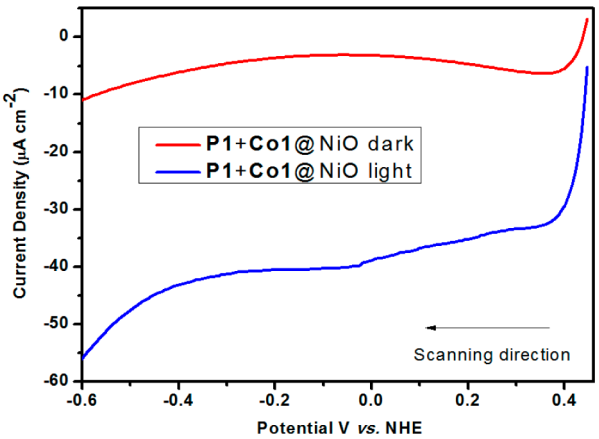

Figure 3. LSV measurements of the WEs under light illumination (light intensity 100 mW cm^{-2}), scan rate = 50 mV s^{-1}, in a **three-electrode** PEC cell with Pt as counter electrode and Ag/AgCl as reference electrode, operated in a 50 mM pH 7.0 phosphate buffer solution.

The transient current responses to on−off cycles show that at −0.2 V vs. Ag/AgCl applied potential the **P1**+**Co1**@NiO photocathode can produce an average photocurrent of ca. −35 μA cm^{-2}, while the reference photocathode **P1**@NiO without the catalyst **Co1** produced only −4 μA cm^{-2} current density under the same condition (Figure 4), while for the **Co1**@NiO electrode, only an indistinct photocurrent can be observed (SI Figure S12). Compared to our previous work where **P1** and $[Co(dmgBF_2)_2(H_2O)_2]$ were encapsulated on an NiO film,[21] the photostability of the present device was significantly improved, which means the phosphonic acid anchoring group in the catalyst **Co1** benefits to the photostability of this PEC device. After 90 min illumination, a photocurrent density of −20 μA cm^{-2} is maintained (SI Figure S13). The photogenerated hydrogen gas was confirmed by GC, 0.082 C charges passed the electrode. 0.29 μmol H_2 was detected, giving a Faraday efficiency of 68%.

With both functional photoanode and photocathode in hand, we have prepared a tandem PEC cell with a two-electrode

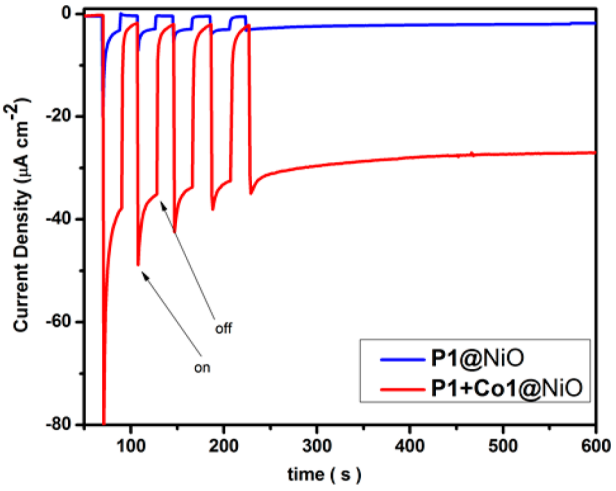

Figure 4. Transient current responses to on−off cycles and full time photocurrent of illumination (light intensity 100 mW cm^{-2}) on photocathodes under an applied potential of −0.2 V vs Ag/AgCl in a **three-electrode** PEC cell with Pt as counter electrode, operated in a 50 mM pH 7.0 phosphate buffer solution.

configuration. The working electrode (WE) is the **P1**+**Co1**@NiO photocathode, and the counter electrode (CE) is the **L0**+**Ru1**@TiO_2 photoanode. The direction of the light illumination on photoelectrode was essential to the performance of the PEC cell. Three configurations were performed by different illumination methods, as shown in Figure 5. In **configuration 1**, both electrodes were simultaneously illuminated, and the best performance was obtained.

When the light is illuminated from the **P1**+**Co1**@NiO side (**configuration 2**), the tandem PEC cell exhibits better performance than that of **configuration 3** where the light is illu-minated from the **L0**+**Ru1**@TiO_2 side. The reason is probably due to the overlap of the absorption regions of **L0** and **P1** (SI Figure S6 and S7). As the TiO_2 film (8 μm) used in this PEC cell is thicker than the NiO film (1 μm), the light can go through NiO film first, and more remaining light can reach the TiO_2 film. Considering that **configuration 1** is the best illumination path for PEC cells in our case, **configuration 1** was therefore selected to test the performances of this tandem PEC cell.

From LSV experiments on the **P1**+**Co1**@NiO/**L0**+**Ru1**@TiO_2 PEC cell, it was found that the photocurrent rapidly increased with the changing of applied potential from 0.8 to 0.6 V (vs. NHE), and reached a plateau at E < 0.6 V with a photocurrent density of ca. −70 μA cm^{-2} (as shown in Figure 6). It is clearly shown that this tandem PEC cell can work without any applied bias. Transient current responses to on−off cycles and full time photocurrent under illumination without bias were studied (Figure 7). First, the photocurrent density of **P1**+**Co1**@NiO/Pt in the two-electrode setup was much lower (5 μA cm^{-2}, Figure 7 blue) than the three-electrode setup one (35 μA cm^{-2}, Figure 4 red). This behavior can be explained as follows, in the two-electrode setup, the valence band of NiO is located around 0.5 V vs NHE, which is not high enough to drive water oxidation, that is why the **P1**+**Co1**@NiO/Pt PEC cell almost does not work in two-electrode setup. While in the three-electrode setup, the Pt counter electrode can get extra potential from the electrochemical workstation for water oxidation. Second, for the tandem cell (**P1**+**Co1**@NiO/**L0**+**Ru1**@TiO_2), the photocurrent density shows a significant

DOI: 10.1021/jacs.5b04856
J. Am. Chem. Soc. 2015, 137, 9153−9159

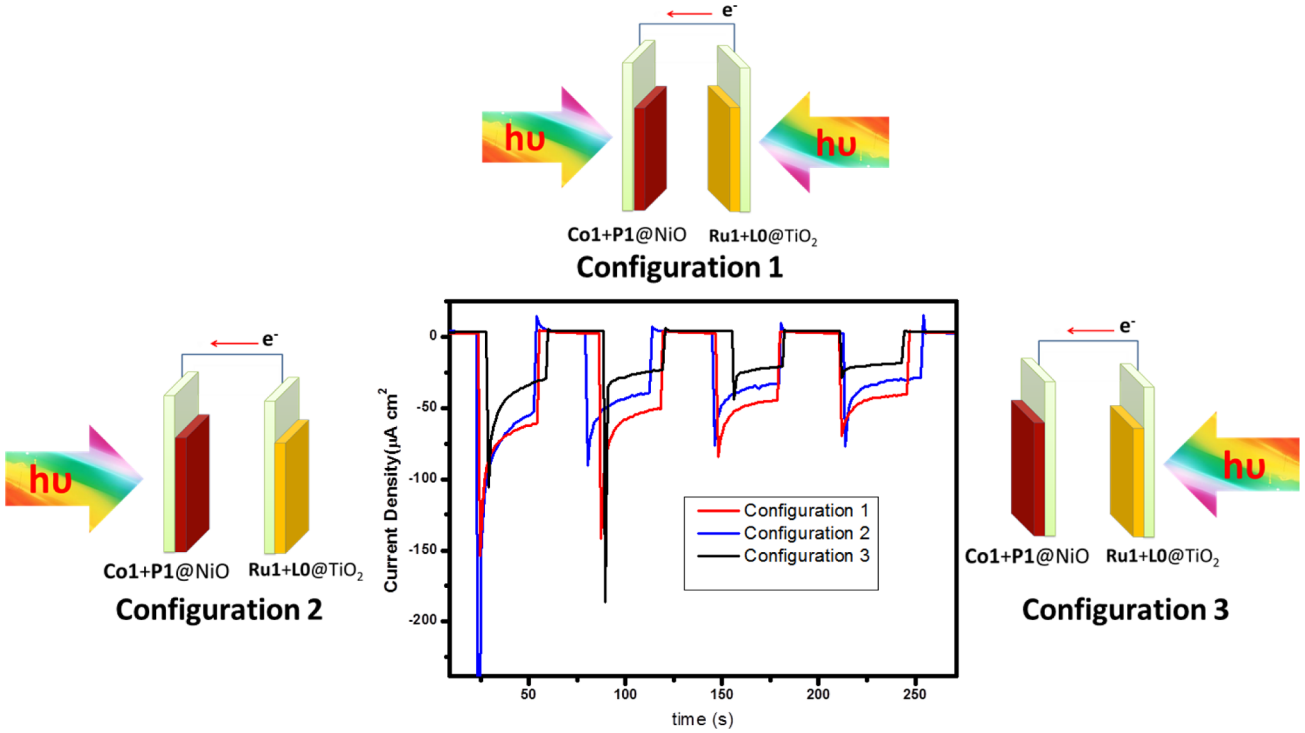

Figure 5. Transient current responses to on−off cycles of a tandem PEC device in **two-electrode** setup with different directions of the light illumination (without any applied potential).

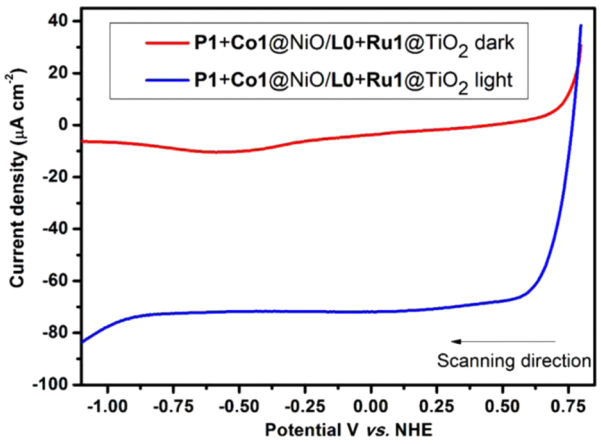

Figure 6. LSV measurements of the WEs under light illumination (light intensity 100 mW cm^{-2}), scan rate = 50 mV s^{-1}, in a **two-electrode** PEC cell as **configuration 1**.

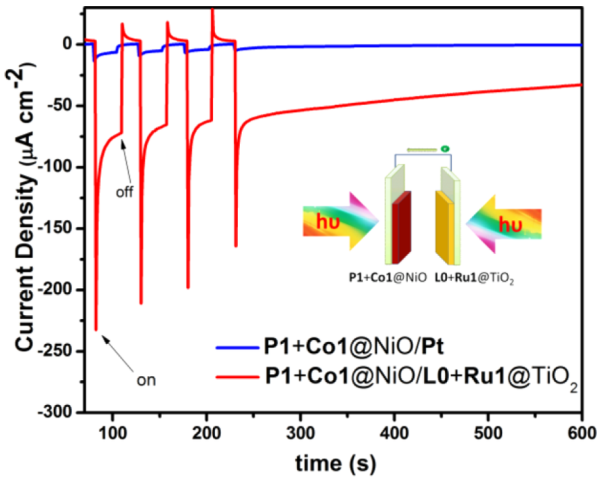

Figure 7. Transient current responses to on−off cycles and full time photocurrent of illumination on photoelectrodes in **two-electrode** setups without any bias, **P1+Co1**@NiO as WE, Pt or **L0+Ru1**@TiO_2 as CE. Operated in a 50 mM pH 7.0 phosphate buffer solution (light intensity 100 mW cm^{-2}).

enhancement (ca. 70 μA cm^{-2}) compared to **P1+Co1**@NiO/Pt. This enhancement was due to the replacement of Pt by the **L0+Ru1**@TiO_2 photoanode, in this case, the photogenerated electrons and holes can flow in this PEC cell, as shown in Scheme 2. The difference between **P1+Co1**@NiO/Pt and **P1+Co1**@NiO/**L0+Ru1**@TiO_2 PEC cells indicates that a good photoanode can not only provide protons for the hydrogen generation half-reaction, but also assist the charge flow between two electrodes, which means that good design of the photoanode is quite necessary and important for tandem PEC cells.

From full time photocurrent measurement on this tandem PEC cell, we found a relatively slow photocurrent decay (ca. 60% photocurrent remained after 10 min illumination). Photogenerated hydrogen was collected and measured by GC from the tandem PEC cell (**P1+Co1**@NiO/**L0+Ru1**@TiO_2) with the two-electrode setup and without external bias for 100 min illumination (using a two-compartment cell divided by a glass frit, as shown in SI Figure S14). A 0.33 μmol portion of H_2 was produced with 0.117 C (SI Figure S15) charge passing through the electrodes, which corresponds to 55% Faraday efficiency. These observed Faraday efficiencies for **P1+Co1**@NiO (in the three-electrode setup) and **P1+Co1**@NiO/**L0+Ru1**@TiO_2 (in the two-electrode setup) are similar to those reported in literature.[27] However, we believe that the Faraday efficiency was underestimated in our case, although two-compartment cell divided by glass frit was used, some of

DOI: 10.1021/jacs.5b04856
J. Am. Chem. Soc. 2015, 137, 9153−9159

the molecular O_2 and H_2 generated in each compartment can be dissolved in the solution, and then diffuse to the other compartment for respective reduction and oxidation, resulting in the low observed Faraday efficiency.

With the Faraday efficiency, the performance of the tandem PEC cell can be assessed by the corresponding solar-to-hydrogen conversion efficiency η_{STH} with eq 1,[28−30] where J_{op} is the effective operating current density measured during device operation (70 μA cm^{-2}), V is the water splitting potential required (1.23 V), V_{bias} is the bias voltage that can be added in series with the two electrodes (0 V), P_{light} is the incident light power (100 mW cm^{-2}), and η_F is the Faraday efficiency (55%). According to eq 1, η_{STH} of this tandem device is calculated to be 0.05%.

$$\eta_{STH} = \frac{(J_{op}[\mathrm{mAcm^{-2}}] \times (V_{\text{water splitting}} - V_{bias}) \times \eta_F)}{P_{light}[\mathrm{mW\,cm^{-2}}]} \quad (1)$$

A monochromatic incident photon-to-electron conversion efficiency (IPCE) measurement was performed, due to the limitation of experimental conditions, the IPCE of **Configuration 1** is very challenging to measure. As shown in Figure 5, **Configuration 2** displays a comparable performance to **Configuration 1**, so the IPCE of this tandem PEC cell was performed by using **Configuration 2**. As shown in Figure 8, the

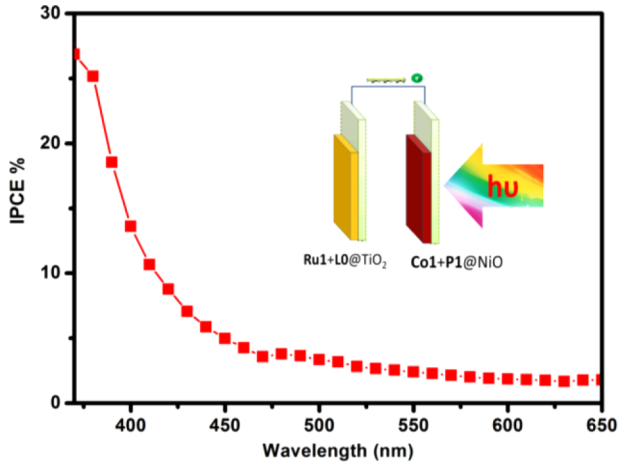

Figure 8. IPEC spectra of **Configuration 2** in 50 mM pH 7 phosphate buffer, in the two-electrode setup without applying any bias voltage (data points are from the average of three independent experiments).

tandem PEC cell (**P1+Co1**@NiO/**L0+Ru1**@TiO_2) shows an IPCE of 25.2% at 380 nm (max_{abs} of **L0**), and 3.9% at 480 nm (max_{abs} of **P1**). This IPCE spectrum indicates that both **L0** and **P1** contribute to the photon-to-electron conversion in this tandem PEC cell, this is an advantage of using the concept of dye-sensitized photoelectrodes with different dyes to achieve a broader absorption of visible light.

It is known that NiO has a poor hole mobility as a p-type semiconductor,[31] and short hole diffusion length, leading to fast charge recombination.[32] At the same time, it is difficult to prepare thicker NiO films to load more dyes and catalysts.[31,33] Our IPCE data also indicates that our photoanode can convert more light into electrons than that of photocathode. And the photocurrent generated by **P1+Co1**@NiO is much lower than that of **L0+Ru1**@TiO_2 (Figures 2 and 4), these indicate that the NiO-based photocathode is the bottleneck of this tandem cell. However, it is believed that with the development of new p-type semiconductors and new routes to prepare thicker films, better PEC devices can be prepared with this type of tandem DS-PEC cell design.

CONCLUSIONS

In summary, an n-type organic dye **L0** coabsorbed with a molecular water oxidation catalyst **Ru1** on TiO_2 was used for preparation of a photoanode, and visible light driven water oxidation using this photoanode was successfully achieved. The photoanode **L0+Ru1**@TiO_2 can produce a remarkable average photocurrent of 300 μA cm^{-2} under pH 7 neutral conditions. A hydrogen generation catalyst **Co1** cosensitized with an organic dye **P1** on NiO was used for a photocathode. Both the photocurrent and the photostability of this photocathode were improved compared to previous reported systems. A tandem DS-PEC cell was designed and prepared by connecting the above-mentioned photoanode and photocathode. For the first time, a metal free organic dye sensitized tandem PEC cell can split water by visible light with IPCE of 25% at 380 nm under neutral pH conditions without bias. These results provide new guidance for the design of molecular PEC cells, leading to great promise for constructing low-cost Pt-free devices for artificial photosynthesis in the future.

ASSOCIATED CONTENT

Supporting Information

Synthesis of molecules, NMR, MS, IR, UV−vis, and electrochemical measurement details. The Supporting Information is available free of charge on the ACS Publications website at DOI: 10.1021/jacs.5b04856.

AUTHOR INFORMATION

Corresponding Author

*lichengs@kth.se

Notes

The authors declare no competing financial interest.

ACKNOWLEDGMENTS

We acknowledge the financial support of this work by the Swedish Energy Agency, the Knut and Alice Wallenberg Foundation, the Swedish Research Council, the National Natural Science Foundation of China (21120102036, 91233201), the National Basic Research Program of China (973 program, 2014CB239402), and the China Scholarship Council.

REFERENCES

(1) Gratzel, M. *Nature* **2001**, *414*, 338.
(2) Walter, M. G.; Warren, E. L.; McKone, J. R.; Boettcher, S. W.; Mi, Q.; Santori, E. A.; Lewis, N. S. *Chem. Rev.* **2010**, *110*, 6446.
(3) Tachibana, Y.; Vayssieres, L.; Durrant, J. R. *Nat. Photonics* **2012**, *6*, 511.
(4) Yagi, M.; Kaneko, M. *Chem. Rev.* **2000**, *101*, 21.
(5) Francàs, L.; Bofill, R.; García-Antón, J.; Escriche, L.; Sala, X.; Llobet, A. In *Molecular Water Oxidation Catalysis*; John Wiley & Sons, Ltd: New York, 2014; p 29.
(6) Duan, L.; Tong, L.; Xu, Y.; Sun, L. *Energy Environ. Sci.* **2011**, *4*, 3296.
(7) Imahori, H. *ChemSusChem* **2015**, *8*, 426.
(8) Yu, Z.; Li, F.; Sun, L. *Energy Environ. Sci.* **2015**, *8*, 760.
(9) Li, L.; Duan, L. L.; Xu, Y. H.; Gorlov, M.; Hagfeldt, A.; Sun, L. C. *Chem. Commun.* **2010**, *46*, 7307.

DOI: 10.1021/jacs.5b04856
J. Am. Chem. Soc. 2015, 137, 9153−9159

(10) Gao, Y.; Ding, X.; Liu, J. H.; Wang, L.; Lu, Z. K.; Li, L.; Sun, L. C. *J. Am. Chem. Soc.* **2013**, *135*, 4219.
(11) Gao, Y.; Zhang, L.; Ding, X.; Sun, L. *Phys. Chem. Chem. Phys.* **2014**, *16*, 12008.
(12) Zhang, L.; Gao, Y.; Ding, X.; Yu, Z.; Sun, L. *ChemSusChem* **2014**, *7*, 2801.
(13) Fan, K.; Li, F.; Wang, L.; Daniel, Q.; Gabrielsson, E.; Sun, L. *Phys. Chem. Chem. Phys.* **2014**, *16*, 25234.
(14) O'Regan, B.; Gratzel, M. *Nature* **1991**, *353*, 737.
(15) Kirner, J. T.; Stracke, J. J.; Gregg, B. A.; Finke, R. G. *ACS Appl. Mater. Interfaces* **2014**, *6*, 13367.
(16) Swierk, J. R.; Méndez-Hernández, D. D.; McCool, N. S.; Liddell, P.; Terazono, Y.; Pahk, I.; Tomlin, J. J.; Oster, N. V.; Moore, T. A.; Moore, A. L.; Gust, D.; Mallouk, T. E. *Proc. Natl. Acad. Sci. U. S. A.* **2015**, *112*, 1681.
(17) Nattestad, A.; Mozer, A. J.; Fischer, M. K. R.; Cheng, Y. B.; Mishra, A.; Bauerle, P.; Bach, U. *Nat. Mater.* **2010**, *9*, 31.
(18) Alessio, E.; Mestroni, G.; Nardin, G.; Attia, W. M.; Calligaris, M.; Sava, G.; Zorzet, S. *Inorg. Chem.* **1988**, *27*, 4099.
(19) Bakac, A.; Espenson, J. H. *J. Am. Chem. Soc.* **1984**, *106*, 5197.
(20) Li, L.; Gibson, E. A.; Qin, P.; Boschloo, G.; Gorlov, M.; Hagfeldt, A.; Sun, L. C. *Adv. Mater.* **2010**, *22*, 1759.
(21) Li, L.; Duan, L.; Wen, F.; Li, C.; Wang, M.; Hagfeldt, A.; Sun, L. *Chem. Commun.* **2012**, *48*, 988.
(22) Hagberg, D. P.; Marinado, T.; Karlsson, K. M.; Nonomura, K.; Qin, P.; Boschloo, G.; Brinck, T.; Hagfeldt, A.; Sun, L. *J. Org. Chem.* **2007**, *72*, 9550.
(23) Qin, P.; Zhu, H.; Edvinsson, T.; Boschloo, G.; Hagfeldt, A.; Sun, L. *J. Am. Chem. Soc.* **2008**, *130*, 8570.
(24) Kitamura, T.; Ikeda, M.; Shigaki, K.; Inoue, T.; Anderson, N. A.; Ai, X.; Lian, T.; Yanagida, S. *Chem. Mater.* **2004**, *16*, 1806.
(25) Liang, Y.; Tsubota, T.; Mooij, L. P. A.; van de Krol, R. *J. Phys. Chem. C* **2011**, *115*, 17594.
(26) Gabrielsson, E.; Tian, H.; Eriksson, S. K.; Gao, J.; Chen, H.; Li, F.; Oscarsson, J.; Sun, J.; Rensmo, H.; Kloo, L.; Hagfeldt, A.; Sun, L. *Chem. Commun.* **2015**, *51*, 3858.
(27) Ji, Z.; He, M.; Huang, Z.; Ozkan, U.; Wu, Y. *J. Am. Chem. Soc.* **2013**, *135*, 11696.
(28) Van de Krol, R.; Schoonman, J. In *Sustainable Energy Technologies*; Hanjalić, K., Van de Krol, R., Lekić, A., Eds.; Springer: Netherlands, 2008; p 121.
(29) van de Krol, R.; Liang, Y.; Schoonman, J. *J. Mater. Chem.* **2008**, *18*, 2311.
(30) Hisatomi, T.; Kubota, J.; Domen, K. *Chem. Soc. Rev.* **2014**, *43*, 7520.
(31) Morandeira, A.; Fortage, J.; Edvinsson, T.; Le Pleux, L.; Blart, E.; Boschloo, G.; Hagfeldt, A.; Hammarström, L.; Odobel, F. *J. Phys. Chem. C* **2008**, *112*, 1721.
(32) Mori, S.; Fukuda, S.; Sumikura, S.; Takeda, Y.; Tamaki, Y.; Suzuki, E.; Abe, T. *J. Phys. Chem. C* **2008**, *112*, 16134.
(33) Lepleux, L.; Chavillon, B.; Pellegrin, Y.; Blart, E.; Cario, L.; Jobic, S.; Odobel, F. *Inorg. Chem.* **2009**, *48*, 8245.

DOI: 10.1021/jacs.5b04856
J. Am. Chem. Soc. 2015, 137, 9153−9159